International Journal of Pharmaceutics 640 (2023) 122990

Contents lists available at ScienceDirect

International Journal of Pharmaceutics

journal homepage: www.elsevier.com/locate/ijpharm

Feasibility of intranasal delivery of thin-film freeze-dried, mucoadhesive vaccine powders

Yu-Sheng Yu [a,f], Khaled AboulFotouh [a], Haiyue Xu [a], Gerallt Williams [b], Julie Suman [c], Chris Cano [d], Zachary N. Warnken [e], Kevin C.-W. Wu [f,g], Robert O. Williams III [a], Zhengrong Cui [a,*]

[a] The University of Texas at Austin, College of Pharmacy, Division of Molecular Pharmaceutics and Drug Delivery, Austin, TX, United States
[b] Aptar Pharma, Le Vaudreuil, France
[c] Aptar Pharma, Congers, NY, United States
[d] TFF Pharmaceuticals, Inc., Fort Worth, TX, United States
[e] Via Therapeutics, Inc., Austin, TX, United States
[f] National Taiwan University, Department of Chemical Engineering, Taipei, Taiwan
[g] National Health Research Institute, Institute of Biomedical Engineering and Nanomedicine, Miaoli, Taiwan

ARTICLE INFO

Keywords:
Vaccine
Powder
Freeze-drying
Nasal
Pediatric
Adult

ABSTRACT

Intranasal vaccination by directly applying a vaccine dry powder is appealing. However, a method that can be used to transform a vaccine from a liquid to a dry powder and a device that can be used to administer the powder to the desired region(s) of the nasal cavity are critical for successful intranasal vaccination. In the present study, using a model vaccine that contains liposomal monophosphoryl lipid A and QS-21 adjuvant (AdjLMQ) and ovalbumin (OVA) as a model antigen, it was shown that thin-film freeze-drying can be applied to convert the liquid vaccine containing sucrose at a sucrose to lipid ratio of 15:1 (w/w) into dry powders, in the presence or absence of carboxymethyl cellulose sodium salt (CMC) as a mucoadhesive agent. Ultimately, the thin-film freeze-dried AdjLMQ/OVA vaccine powder containing 1.9% (w/w) of CMC (i.e., TFF AdjLMQ/OVA/$CMC_{1.9\%}$ powder) was selected for additional evaluation because the TFF AdjLMQ/OVA/$CMC_{1.9\%}$ powder was mucoadhesive and maintained the integrity of the antigen and the physical properties of the vaccine. Compared to the TFF AdjLMQ/OVA powder that did not contain CMC, the TFF AdjLMQ/OVA/$CMC_{1.9\%}$ powder had a lower moisture content and a higher glass transition temperature. In addition, the TFF AdjLMQ/OVA/$CMC_{1.9\%}$ thin films were relatively thicker than the TFF AdjLMQ/OVA thin films without CMC. When sprayed with Aptar Pharma's Unidose Powder Nasal Spray System (UDSP), the TFF AdjLMQ/OVA powder and the TFF AdjLMQ/OVA/$CMC_{1.9\%}$ powder generated similar particle size distribution curves, spray patterns, and plume geometries. Importantly, after the TFF AdjLMQ/OVA/$CMC_{1.9\%}$ powder was sprayed with the UDSP nasal device, the integrity of the OVA antigen and the AdjLMQ liposomes did not change. Finally, a Taguchi L4 orthogonal array was applied to identify the optimal parameters for using the UDSP device to deliver the TFF AdjLMQ/OVA/$CMC_{1.9\%}$ powder to the middle and lower turbinate and the nasopharynx regions in both adult and child nasal replica casts. Results from this study showed that it is feasible to apply the thin-film freeze-drying technology to transform a nasal vaccine candidate from liquid to a dry powder and then use the UDSP nasal device to deliver the vaccine powder to the desired regions in the nasal cavity for intranasal vaccination.

1. Introduction

Intranasal vaccination is an attractive, non-invasive route of vaccine administration. Intranasal vaccines can induce specific immune responses not only systemically, but also in the mucosal secretions of the respiratory tract (Birkhoff et al., 2009), which is advantageous as many pathogens infect their hosts through the respiratory tract (Chavda et al., 2021). In fact, several nasal vaccines have been approved for human use around the world, including the FluMist Quadrivalent in the United States (US) (Suryadevara and Domachowske, 2014), Fluenz Tetra in the

* Corresponding author.
E-mail address: Zhengrong.cui@austin.utexas.edu (Z. Cui).

https://doi.org/10.1016/j.ijpharm.2023.122990
Received 5 February 2023; Received in revised form 21 April 2023; Accepted 24 April 2023
Available online 29 April 2023

European Union (EU) (Gasparini et al., 2021), NASOVAC-S in India (Ortiz et al., 2015), a freeze-dried nasal live influenza vaccine (Ganwu®) by the Changchun BCHT Biotechnology in China, and more recently a nasal Coronavirus disease 2019 (COVID-19) vaccine by Bharat Biotech in India. Those nasal vaccines are live (attenuated) influenza virus-based or adenovirus-based and are presented as a liquid suspension or a freeze-dried powder for reconstitution. The liquid vaccine suspension is then administered intranasally using a nasal spray system such as the BD Accuspray™. However, intranasal administration of vaccine directly as a dry powder has advantages, including ease of storage and distribution (Flood et al., 2016), extended residence time in the nasal cavity, and a higher dose of vaccine that can be administered. Unfortunately, vaccine dry powders with the proper aerosol properties for deposition in the desired region(s) in the nasal cavity and a method to prepare the dry powders remain needed.

Thin-film freeze-drying is a bottom-up dry powder engineering technology. It involves the ultra-rapid thin-film freezing (TFF) of a liquid (e.g., solution, suspension, or emulsion) on a cryogenically cooled solid surface (Engstrom et al., 2008; Overhoff et al., 2009). The liquid is dropped as droplets (e.g., 2 mm in diameter) from about 1 cm to 10 cm above the cryogenically cooled solid surface. Upon impact, the droplet rapidly spreads into a thin film on the cooled surface, which is then frozen. Solvent such as water in the frozen thin films is removed by lyophilization. Dry powder engineering using the TFF technology is advantageous over other similar dry powder engineering technologies such as conventional shelf freeze-drying, spray drying, and spray freeze-drying in that it avoids or minimizes shear stress and heat stress, while generating powders that are generally highly porous, brittle (Hufnagel et al., 2022), and have a large specific surface area (Wang et al., 2021), making them suitable for pulmonary delivery. However, the TFF process is associated with a relatively larger liquid–solid interface between the liquid droplets and the cryogenically cooled solid surface and between liquid and ice. Previously, it has been shown that the TFF technology can be applied to produce dry powders of various vaccines, including vaccines adjuvanted with aluminum salts (Alzhrani et al., 2021; Li et al., 2015; Thakkar et al., 2018), (nano)emulsions such as MF59 or AddaVax (AboulFotouh et al., 2022a), and liposomes such as $AS01_B$ (AboulFotouh et al., 2022b).

Herein, a model vaccine comprised of ovalbumin (OVA) as an antigen and a liposomal adjuvant was used to test the feasibility of using the TFF technology to prepare vaccine dry powders for direct intranasal administration. All currently approved human nasal vaccines are virus-based and do not contain any adjuvant. A liposomal adjuvant, AdjLMQ, with composition identical to $AS01_B$, but prepared with a different method in our laboratories and in a different buffer, was chosen in this study because a recent report from our group showed that the $AS01_B$-containing Shingrix vaccine can be converted to dry powders by thin-film freeze-drying (AboulFotouh et al., 2022b). Results from a recent study have also demonstrated the safety and efficacy of $AS01_B$ as a potential nasal vaccine adjuvant in a mouse model (Sato-Kaneko et al., 2022). Moreover, the adjuvant activity of MPL or QS-21 alone after intranasal administration has been documented (Baldridge et al., 2000; Sasaki et al., 1998a; Sasaki et al., 1998b).

To increase the residence time of the vaccine in the nasal cavity, various mucoadhesive agents have been included in the AdjLMQ/OVA vaccine formulation, and their effect on the vaccine was studied. The mucoadhesive agents studied include chitosan, sodium alginate, gelatin, and sodium carboxymethylcellulose (CMC), each with its own unique mechanism(s) of interaction with the mucosa (Dekina et al., 2016; Grabovac et al., 2005; Kesavan et al., 2010; Sogias et al., 2008). A challenge is that the mucoadhesive agent may interact with the AdjLMQ/OVA vaccine. Therefore, the effect of different mucoadhesive agents on the physical properties of the AdjLMQ/OVA vaccine before and after the vaccine was subjected to thin-film freeze-drying with sucrose as an excipient was studied. CMC at a concentration that showed minimal effect on the physical properties of the AdjLMQ/OVA vaccine was chosen for further characterization. The particle size distribution, spray pattern, and plume geometry of selected AdjLMQ/OVA vaccine powders were studied after actuation using Aptar Pharma's Unidose Powder Nasal Spray System (UDSP). Finally, the deposition patterns of a selected AdjLMQ/OVA vaccine powder following actuation using the UDSP nasal device into 3D printed nasal replica casts based on the CT-scan images of the noses of an adult and a child were evaluated to predict the feasibility of using the UDSP nasal device to deliver thin-film freeze-dried vaccine powders (TFF vaccine powders) directly into the posterior nasal cavity, especially the nasopharynx region, of the human nasal cavity (Warnken et al., 2018). Unlike in infants, in children older than two years and in adults, the Waldeyer's ring in the naso-oropharynx region is the key lymphoid tissue in the nasal cavity (Davis, 2001; Debertin et al., 2003). Therefore, for an intranasal vaccine to induce specific immune responses, the vaccine needs to be delivered either directly to the nasopharynx region or to the posterior nasal cavity and then move by means of ciliary clearance to the naso-oropharynx region following the mucous blanket posterior movement. Within the posterior nasal cavity, delivery of the vaccine to the upper turbinate region, where the olfactory bulb resides, should be avoided or minimized to reduce the access of the vaccine to the brain via the olfactory nerves (Cai et al., 2022; Xu et al., 2021b).

2. Materials and methods

2.1. Materials

Albumin from chicken egg white (ovalbumin, OVA), CMC low viscosity, MPL from *Salmonella enterica* serotype minnesota Re 595 (Re mutant), porcine mucin type III, and 2-mercaptoethanol were from Sigma-Aldrich (St. Louis, MO). QS-21 was from Dessert King International (San Diego, CA). Sucrose was from Millipore (Billerica, MA). Anhydrous ethanol (EtOH) was from Decon Labs (King of Prussia, PA). Cholesterol was from MP Biomedicals (Santa Ana, CA). The 1,2-dioleoyl-*sn*-glycero-3-phosphocholine (DOPC) was from Avanti Polar Lipids, Inc. (Alabaster, AL). Fluorescein isothiocyanate isomer I (FITC) was from Acros Organics (Geel, Belgium). Dulbecco's phosphate-buffered saline (DPBS, pH 7.0–7.3, 9.5 mM) was from Gibco (Grand Island, NY). Laemmli sample buffer 4 × and Coomassie G-250 were from Bio-Rad (Hercules, CA). Blue prestained protein standard was from New England Biolabs (Ipswich, MA). Artificial nasal mucus was from Biochemazone (Leduc, Alberta, Canada). HYDRANAL™-Coulomat AG was from Honeywell (Charlotte, NC). The UDSP nasal devices were provided by the Aptar Pharma (Le Vaudreuil, France). All chemicals were used as received.

2.2. Preparation of the AdjLMQ/OVA model vaccine

$AS01_B$ is an adjuvant in Shingrix (Zoster vaccine recombinant, Adjuvanted). In the present study, we prepared AdjLMQ based on the composition of $AS01_B$ mentioned in the Shingrix Prescribing Information (https://www.fda.gov/media/108597/download). To prepare the AdjLMQ/OVA model vaccine, the liposomal adjuvant was prepared first as described before (AboulFotouh et al., 2022b). Briefly, 1.25 mL of ethanol containing 4.0 mg of DOPC, 1.0 mg of cholesterol, and 0.2 mg of MPL was placed in a glass vial. A lipid membrane was formed in the vial by evaporating the ethanol under gentle nitrogen flow. Next, 0.5 mL of DPBS was added to the vial to rehydrate the lipids, and the mixture was stirred overnight at room temperature. The final concentration of DOPC in the liposome suspension was 8 mg/mL. The liposome suspension was sonicated with a probe sonicator (Qsonica Q700) until the Z-average particle size reached about 100 nm based on dynamic light scattering (DLS). The AdjLMQ/OVA model vaccine was prepared by adding the stock solutions containing 19.5 mg of sucrose, 50 μg of OVA, and 50 μg of QS-21 to 125 μL of the liposome suspension, and the final volume was adjusted to 500 μL with DPBS.

2.3. Preparation of AdjLMQ/OVA model vaccines with CMC

To prepare the AdjLMQ/OVA model vaccine with different concentrations of CMC, the stock solutions containing 19.5 mg of sucrose, 50 μg of OVA, and 50 μg of QS-21 were first added to 125 μL of liposome suspension, followed by different volumes of a CMC in DPBS solution (2%, w/v). The final volume was then adjusted to 500 μL to achieve a final CMC concentration of 0.1%, 0.2%, 0.4%, or 1%, w/v, corresponding to 1.9%, 3.7%, 7.2%, or 16.3% (w/w) of the CMC to the total weight of all components in the vaccine formulation except water.

2.4. Thin-film freeze-drying of the AdjLMQ/OVA model vaccines

The as-prepared AdjLMQ/OVA vaccines, with or without CMC, were converted into dry powders by thin-film freeze-drying. First, the liquid vaccines were frozen into small thin films following the reported single-vial TFF process (Xu et al., 2021a). Briefly, a glass vial was placed on dry ice until the temperature reached equilibrium. The liquid vaccine was added dropwise with a BD 1 mL syringe with a 21G needle to the bottom of the vial to form frozen thin films. The frozen films were then freeze-dried in a lyophilizer (SP VirTis AdVantage Pro). The lyophilization cycle was −40 °C for 20 h, gradually ramping from −40 °C to 25 °C over 20 h, and then 25 °C for 20 h. The chamber pressure was maintained at 80 mTorr throughout the lyophilization process. After lyophilization, the vials were backfilled with nitrogen gas, capped, crimped, and stored at room temperature.

2.5. Determination of particle size and zeta potential

A Malvern Nano ZS (Westborough, MA) was used to measure the particle size and zeta potential of the liposomes and the vaccines. The vaccine powder was reconstituted with deionized water (DI water) at a volume identical to the volume of the liquid vaccine before it was subjected to thin-film freeze-drying. Samples were diluted 50 times with DPBS. For the liquid vaccines (i.e., before being subjected to thin-film freeze-drying), the diluted samples were allowed to equilibrate at room temperature for at least 30 min. For the reconstituted vaccines, the samples were diluted and allowed to equilibrate at room temperature overnight to improve the dissolution of CMC. The final pH values of the samples ranged from 7.12 to 7.34.

2.6. Evaluation of the integrity of the OVA and the liposomes

Sodium dodecyl sulfate–polyacrylamide gel electrophoresis (SDS-PAGE) was applied to evaluate the integrity of OVA in AdjLMQ/OVA vaccines before and after they were subjected to thin-film freeze-drying, as well as before and after the vaccine powders were sprayed with an Aptar UDSP nasal device. Vaccine powders were reconstituted with water. To spray a powder, the powder was filled into a UDSP nasal device following the manufacturer's instruction and sprayed into a glass test tube. The powder was then dissolved with water within the test tube. For SDS-PAGE analysis, the sample was mixed with Laemmli sample buffer 4 × containing 10% 2-mercaptoethanol, boiled for 10 min at 100 °C, and then loaded into a well of a 4–20% precast polyacrylamide gel from Bio-Rad (Hercules, CA) (30 μL per well). The blue prestained protein standard was also loaded to the gel. The electrophoresis was performed at 90 V for 90 min. The SDS-PAGE gel was stained with Coomassie G-250, and the gel image was captured with a camera.

Scanning transmission electron microscope (STEM) was utilized to examine the integrity of the liposomes after the vaccine powder was sprayed using a UDSP nasal device. The powder was sprayed into a glass pipette rubber head. The vaccine powder was then reconstituted with water and further diluted 5 times with water and then transferred to a glow discharge-treated, carbon coated copper grid from Electron Microscopy Sciences (Hatfield, PA). The sample was stained with a 2% w/v uranyl acetate solution for 3 min and then air dried. Finally, the STEM images were captured using a Hitachi S5500 (Tokyo, Japan) available in the Texas Materials Institute at UT Austin.

2.7. In vitro mucoadhesion test

The *in vitro* mucoadhesion test was done following a previously reported procedure with modifications (Trenkel and Scherließ, 2021). To simulate the human nasal mucosal tissue, 100 mm square Petri dishes were coated with 1.5% (w/v) agar plus 2% (w/v) porcine mucin in DPBS (pH 6). The coating layer was solidified by incubating the Petri dishes for 2 h at room temperature. The dishes were then stored at 4 °C. To track the movement of the TFF AdjLMQ/OVA thin films on the agar gel, 25 μL of the DPBS was replaced with 25 μL of DPBS containing crystal violet (1% w/v) when preparing the vaccine. To make each film with a similar geometry, the distance between the needle and the bottom of the vial was fixed, and the number of droplets per vial was limited to 5 when performing TFF.

The coated dishes were incubated at 32 °C in a Fisher Scientific incubator-shaker (Hampton, NH) until equilibrium (shaking not applied), and the thin films prepared using thin-film freeze-drying were gently placed onto the gel (1 film per spot). The dishes were then turned vertically and incubated for 10 min at 32 °C. The maximum downward movement of the vaccine film was measured using a ruler.

2.8. Characterization of the vaccine powders

TFF AdjLMQ/OVA vaccine films were prepared for surface profile analysis and scanning electron microscope (SEM) analysis. The surface profiles of the thin films were measured with a Keyence VK-X1100 profilometer (Osaka, Japan) available at UT Austin. Before the measurement, a vaccine thin film was placed onto the unpolished side of the silicon wafer with the top up. The 3D reconstructed images of the film were captured with a 2.5 × objective lens while the ring light source was utilized. The thickness of the film was calculated with the Keyence Multi File Analyzer software. To obtain the SEM images, a film of the TFF AdjLMQ/OVA or the TFF AdjLMQ/OVA with 1.9% CMC was placed onto the conductive carbon tape. The sample was then sputtered with a layer of Au/Pd (60:40) (40 mA, 1 min). SEM images were taken using a Hitachi S5500 with an acceleration voltage of 20 kV.

The residual water content in vaccine powder was determined by Karl Fischer titration using a Mettler Toledo C20 coulometer (Columbus, OH). Briefly, 2.5 mL of Coulomat AG solution was drawn from the solution tank and injected into the vial containing the powder with a gas-tight syringe. The solution was mixed well with the powder, and 2.0 mL of the mixture was then injected back to the solution tank. The amount of water in the samples was then determined using the instrument, and the water content (% w/w) in the samples was calculated with equation (1):

$$\text{Water content } (\%) = \frac{\text{Amount of water (mg)}}{\text{Weight of the sample (mg)}} \times 100 \quad (1)$$

Temperature-modulated differential scanning calorimetry (mDSC) was performed using a TA Instruments Q20 differential scanning calorimeter (New Castle, DE) available at UT Austin. Briefly, 3–5 mg of the powder was loaded to the Tzero hermetic pan from TA Instruments. The scanning range was from −20 to 250 °C. The temperature was modulated ± 1.0 °C every 60 s. The data were analyzed with the TA Instruments TRIOS software.

2.9. Plume geometry, spray pattern, and the particle size distribution of the aerosolized powder

The spray pattern and plume geometry of the TFF vaccine powders were captured with a custom built laser sheet system (Warnken et al., 2018). To study the plume geometry of a vaccine powder, the powder

was loaded into a UDSP nasal spray device and sprayed upward. Images were captured with a camera at a rate of 500 frames per second. To identify the boundary of the plume, the Fiji software (https://imagej.net/software/fiji) was used to create z-stacking images from different time points (a total of 11 frames) to measure the plume angle. For the spray pattern, the vaccine powder was loaded into a UDSP nasal device and sprayed upward, and the laser sheet was located 6 cm above the tip. The images were captured at an angle about 45° and a frame rate of 500 frames per second. The Fiji software was then used to create the z-stacking images from different time points (a total of 11 frames), and the perspective correction of the images was performed with MATLAB R2022a software. The ovality and the area were then measured with the Fiji software.

To measure the particle size distribution of the sprayed vaccine powder, the powder was filled into a UDSP nasal device and sprayed to measure the particle size with a Malvern Spraytec Instrument. During the experiment, the device was fixed with a clamp, and the angle was adjusted to 30° above the horizontal plane. The distance between the tip and the laser spot was 6 cm, while the device to lens distance was 9 cm. The device was actuated manually, and the laser diffraction signal was recorded at a frame rate of 2500 Hz.

SEM was also utilized to examine the particles after the vaccine powder was sprayed with a UDSP nasal device. The SEM specimen mount was first covered with a non-porous carbon tape. The vaccine powder was then sprayed onto the carbon tape at a distance of 6 cm. The sample was then sputtered with Au/Pd (60:40) (40 mA, 1 min), and the images were captured with an acceleration voltage of 20 kV.

2.10. Deposition pattern of the TFF vaccine powder

For this experiment, FITC-labeled OVA (i.e., OVA-FITC) was used to prepare the AdjLMQ/OVA-FITC vaccine with 1.9% CMC. The OVA-FITC was synthesized following a reported method with modifications (i.e., the reaction time was increased to overnight, and the purification was done using ultrafiltration) (Sigma-Aldrich, 2021).

The two 3D-printed nasal casts based on the CT-scan images of a 48-year-old male and a 7-year-old female were used to perform the deposition test (Warnken et al., 2018). The inner surface of the nasal cast was coated with an artificial nasal mucus, and the excess fluid was purged with air. To collect the powder passing beyond the nasal cavity, a 2-μm glass microfiber syringe filter from Cytiva (Marlborough, MA) was attached behind the nasopharynx part. The TFF AdjLMQ/OVA/$CMC_{1.9\%}$ vaccine powder (OVA labeled with FITC) was loaded into a UDSP nasal device and sprayed into the left nostril of the nasal cast. The coronal angle and sagittal angle were 0° or 20° and 45° or 60°, respectively. The definitions of the coronal angle and the sagittal angle are shown in **Fig. S1**. The insertion depth was 0.5 cm for the 48-year-old male nasal cast and 0.4 cm for the 7-year-old female nasal cast. To determine the effect of breathing on the deposition pattern, the nasal cast was connected to a vacuum pump to evaluate the effect of flow rate on the deposition pattern. The flow rate was set at 0 or 10 litters per min (LPM) for the 48-year-old male nasal cast and 0 or 5 LPM for the 7-year-old nasal cast. For three parameters (i.e., coronal angle, sagittal angle, and flow rate), each with 2 levels, the Taguchi L4 orthogonal array (Table 1) was used to find their optimal combination.

After the powder was sprayed, the nasal cast was disassembled into the following parts: (1) vestibule, (2) upper turbinate, (3) middle turbinate, (4) lower turbinate, (5) nasopharynx, and (6) filter. Each part was rinsed with 5 mL of water. The fluorescence intensities of the solutions were measured with a BioTek Microplate Reader (Winooski, VT). The amount of powder deposited in each part was calculated based on a calibration curve constructed with FITC-labeled vaccine powder dissolved in water.

The delivery efficiency of the powder using the UDSP nasal device was calculated based on equation (2):

$$\text{Delivery efficiency } (\%) = \frac{\text{Amount of the powder delivered (mg)}}{\text{Amount of the powder loaded in the UDSP (mg)}} \times 100 \quad (2)$$

The recovery percentage of the vaccine powder in the nasal cast was defined as:

$$\text{Recovery percentage } (\%) = \frac{\text{Total amount of the powder recovered (mg)}}{\text{Amount of the powder delivered (mg)}} \times 100 \quad (3)$$

Where the total amount of the powder recovered was based on the fluorescence intensity measurement.

The deposition efficiency of the vaccine powder in a specific part or region of the nasal cast was defined as:

$$\text{Deposition efficiency } (\%) = \frac{\text{Amount of the powder recovered in each part (mg)}}{\text{Total amount of the powder recovered (mg)}} \times 100 \quad (4)$$

Finally, the total amount of the powder recovered in the desirable region (i.e., middle turbinate, lower turbinate, and nasopharynx region) was defined as the regional deposition efficiency (RDP).

To identify the optimized conditions for the RDP, the signal to noise (S/N) ratio (equation (5)) was calculated for each parameter at different levels based on the larger-the-better characteristic of the Taguchi method (Ghani et al., 2004).

$$\text{S/N ratio} = -10 \times \log\left(\frac{1}{n}\sum_{i=1}^{n}\left(\frac{1}{y_i^2}\right)\right) \quad (5)$$

Where n is the number of replications for each combination, and y is

Table 1
The Taguchi L4 orthogonal array for studying the deposition patterns of the TFF vaccine powder in two different nasal casts.

Run #	Coronal Angle	Sagittal Angle	Flow Rate (LPM)	
			48-year-old	7-year-old
1	0°	45°	0	0
2	20°	60°	0	0
3	20°	45°	10	5
4	0°	60°	10	5

the observed data (i.e., RPD). The mean of S/N ratio was then calculated for each parameter.

2.11. Statistical analysis

Statistical analysis was performed with Microsoft Office Excel. Two-tailed independent Student's *t*-test (equal variance and/or unequal variance) were performed. Data are presented as mean ± standard deviation (S.D.), and the number of the replication (n) was indicated in the figure caption.

3. Results and discussion

3.1. Preparation and thin-film freeze-drying of the AdjLMQ/OVA model vaccine

AdjLMQ was prepared by adding QS-21 to preformed liposomes comprised of DOPC, cholesterol, and MPL (1:0.25:0.05, w/w) (AboulFotouh et al., 2022b). The DOPC/cholesterol/MPL liposomes prepared had a hydrodynamic diameter of 101.3 ± 4.7 nm (n = 9). The AdjLMQ/OVA vaccine was then prepared by mixing the liposome suspension with an OVA solution and a QS-21 solution. Data from a previous study from our group showed that sucrose at a sucrose to lipid ratio of 15:1 (w/w) protected the AdjLMQ/OVA vaccine during thin-film freeze-drying (AboulFotouh et al., 2022b). Fig. 1**A** shows the particle size of the AdjLMQ/OVA vaccine before and after it was subjected to thin-film freeze-drying and reconstitution, and no particle aggregation was observed after the vaccine was subjected to thin-film freeze-drying.

3.2. Preparing AdjLMQ/OVA vaccine formulations with CMC

A mucosal adhesive agent can help increase the residence time of a vaccine in the nasal cavity (Saito et al., 2016), and we tested the compatibility of the AdjLMQ/OVA vaccine with four different, known mucoadhesive agents, CMC, chitosan, gelatin, or sodium alginate, before and after being subjected to thin-film freeze-drying. Both CMC and gelatin were potentially compatible with AdjLMQ/OVA, but CMC, not gelatin, was chosen for further studies because gelatin is a protein product, making it challenging to characterize the protein antigens. CMC was added into the AdjLMQ/OVA vaccine to reach a final concentration of 0, 1.9%, 3.7%, 7.2%, or 16.3% w/w (vs. total weight of the vaccine except water). The addition of CMC in the AdjLMQ/OVA vaccine did not significantly affect the particle size of the vaccine (Fig. 1**A**) but led to an overall reduction in the zeta potential values (Fig. 1**B**), likely due to the ionized carboxyl groups in the CMC. After the vaccines were subjected to thin-film freeze-drying, the particle sizes in the formulations containing 1.9% or 3.7% (w/w) of CMC were similar to their original sizes and the polydispersity index values were about 0.2. Therefore, the AdjLMQ/OVA vaccine formulations with 1.9% or 3.7% of CMC were chosen for additional studies. The AdjLMQ/OVA vaccine formulation with 7.2% (w/w) of CMC was not studied further because the polydispersity index value of the vaccine after being subjected to thin-film freeze-drying and reconstitution became close to 0.3. As to the AdjLMQ/OVA vaccine formulation with 16.3% (w/w) of CMC, the average particle size almost doubled after being subjected to thin-film freeze-drying (Fig. 1**A**). The zeta potential values of the AdjLMQ/OVA vaccines became more negative after they were subjected to thin-film freeze-drying (Fig. 1**B**), but the underlying reason remains unclear.

3.3. In vitro mucoadhesion test

Petri dishes coated with 1.5% (w/v) agar plus 2% (w/v) porcine mucin were used to simulate the surface of human mucosal tissue. In the *in vitro* mucoadhesion test, films of TFF AdjLMQ/OVA powders with 0, 1.9, or 3.7% w/w of CMC and about 1% w/w of crystal violet were placed on the agar plus porcine mucin layer. The dishes were turned vertically and incubated at 32 °C (Fig. 2**A**). The thin films swelled due to the moisture in the gel or the atmosphere and moved down slowly. The maximum traveling distances of the formulations at 10 min were then recorded. Fig. 2**B** shows the downward movement of all three TFF vaccine powders. Only the TFF AdjLMQ/OVA powders without CMC moved (8.1 ± 3.3 mm) after 10 min of incubation. The TFF AdjLMQ/OVA powders with 1.9% or 3.7% w/w CMC did not move, indicating that they were adhesive to the porcine mucin-containing agar surface. Considering there is no difference between TFF AdjLMQ/OVA vaccine with 1.9% and 3.7% w/w CMC (Fig. 2**B**), the AdjLMQ/OVA with 1.9% CMC (AdjLMQ/OVA/$CMC_{1.9\%}$) was selected for further studies.

3.4. The integrity of the OVA before and after the AdjLMQ/OVA vaccine formulations were subjected to thin-film freeze-drying

To evaluate the impact of the thin-film freeze-drying process on the integrity of OVA antigen, SDS-PAGE was used to analyze the AdjLMQ/OVA vaccine formulations containing 0 or 1.9% CMC. The original OVA in solution (Fig. 3, lane I) showed two bands around 43 kDa. Similar doublet bands were found by others (Covaciu et al., 2004; ThermoFisher Scientific, n.d.), which might be attributed to the presence of different glycosylated forms (ThermoFisher Scientific, n.d.). A close comparison of Fig. 3 lanes II vs. IV, and lanes III vs. V did not show any apparent difference, indicating that the integrity of OVA was maintained after being subjected to thin-film freeze-drying, regardless of the presence of the CMC in the vaccine formulations. SDS-PAGE analysis with the individual component of the AdjLMQ/OVA vaccine formulations confirmed that the broad bands below 11 kDa shown in the AdjLMQ/OVA samples (Fig. 3) were from the liposomes (**Fig. S2**).

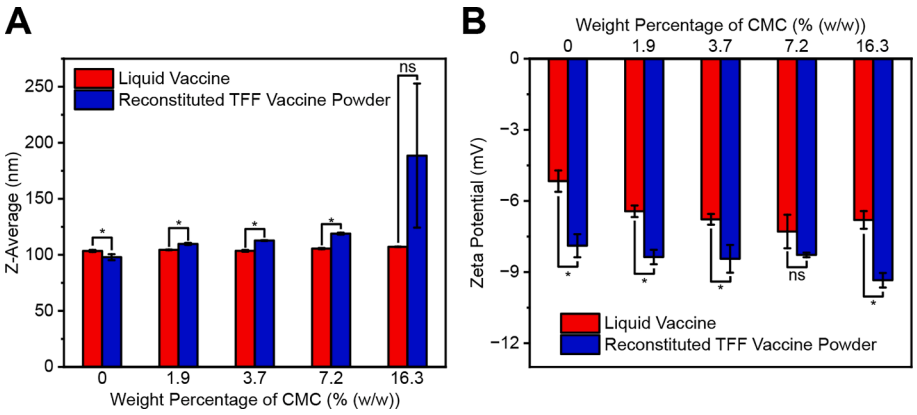

Fig. 1. AdjLMQ/OVA with different concentrations of CMC as a mucoadhesive agent. Shown are (A) particle size and (B) zeta potential before and after the vaccines were subjected to thin-film freeze-drying and reconstitution. Data are mean ± S.D. (n = 3). Two-tailed independent Student's *t*-test (equal variance and unequal variance) were applied to compare the Liquid Vaccine and the Reconstituted TFF Vaccine Powder. ns: non-significant, *p ≤ 0.05. The equality of variances was evaluated using *F*-test with an one-tailed significance level of 0.025.

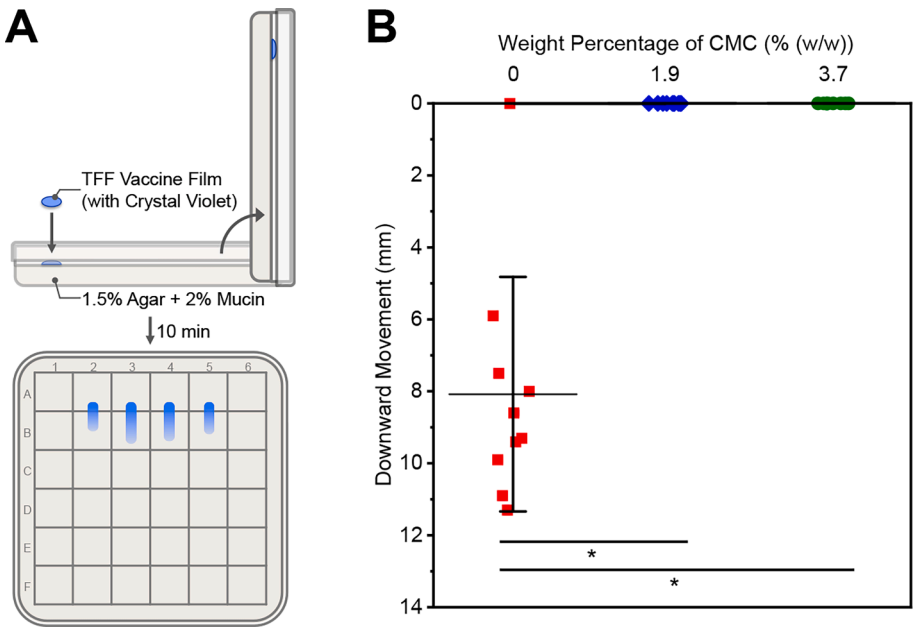

Fig. 2. In vitro mucoadhesion test. (A) Experimental design. (B) Downward movement of TFF AdjLMQ/OVA vaccine powders with 0, 1.9 or 3.7% w/w CMC on 1.5% agar plus 2% porcine mucin gel (bars). Data are mean ± S.D. (n = 10). Data in B were analyzed using two-tailed independent Student's *t*-test (assuming unequal variance) to compare the TFF Vaccine Powder containing CMC with the TFF Vaccine Powder without CMC. * $p \leq 0.05$.

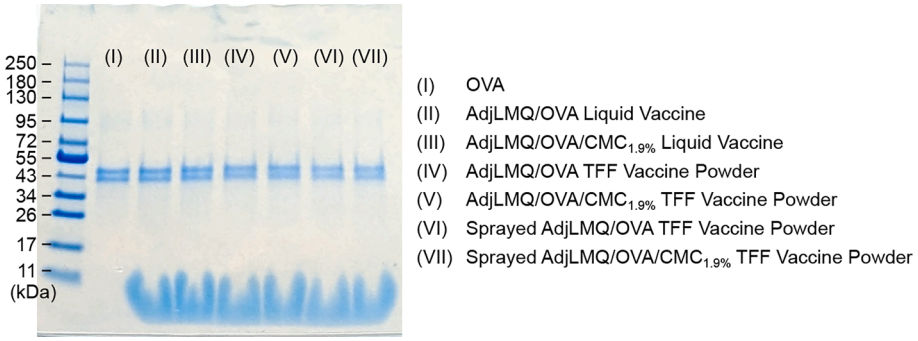

Fig. 3. SDS-PAGE image of OVA alone (I), AdjLMQ/OVA liquid vaccines (II, III), TFF vaccine powders (IV, V), and sprayed TFF vaccine powders (VI, VII) containing 0 or 1.9% w/w of CMC.

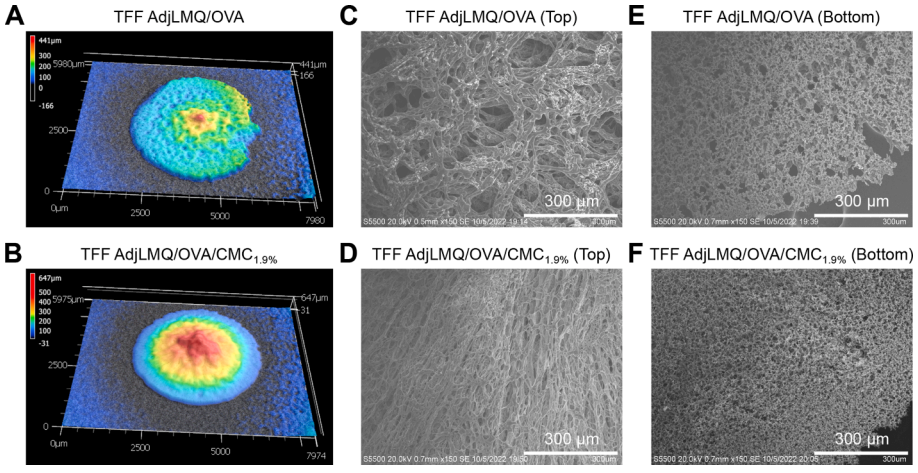

Fig. 4. Characterization of TFF AdjLMQ/OVA and AdjLMQ/OVA/$CMC_{1.9\%}$ films. Shown in A-B are representative surface profiles of the TFF AdjLMQ/OVA (A) and TFF AdjLMQ/OVA/$CMC_{1.9\%}$ films (B). (C-D) Representative SEM images (top view) of the TFF AdjLMQ/OVA (C) and AdjLMQ/OVA/$CMC_{1.9\%}$ films (D). (E-F) Representative SEM images (bottom view) of the TFF AdjLMQ/OVA (E) and AdjLMQ/OVA/$CMC_{1.9\%}$ films (F).

3.5. Characterization of the TFF AdjLMQ/OVA vaccine powders with 0 or 1.9% w/w CMC

The residual water content in the TFF vaccine powders is important to their stability and aerosol properties. The moisture content in the TFF AdjLMQ/OVA and the TFF AdjLMQ/OVA/$CMC_{1.9\%}$ powders were 4.29 ± 0.13% and 2.71 ± 0.21%, respectively. The CMC in the TFF AdjLMQ/OVA/$CMC_{1.9\%}$ sample likely made the sucrose matrix less hygroscopic.

Surface profilometer was used to characterize the surface of the TFF vaccine powders. Fig. 4**A and 3B** show the images of the thin films of TFF AdjLMQ/OVA powders with 0 or 1.9% w/w of CMC. It appears that the TFF AdjLMQ/OVA film was more porous compared to the TFF AdjLMQ/OVA/$CMC_{1.9\%}$ film. In addition, the TFF AdjLMQ/OVA/$CMC_{1.9\%}$ film had a radial pattern, likely because the nucleation or the growth of the sucrose matrix were altered by the CMC during the TFF process. The mean thickness of the TFF films was determined using seven randomly selected films. The mean thickness of the TFF AdjLMQ/OVA/$CMC_{1.9\%}$ films was 208.7 ± 51.1 μm, about 25% larger than that of the TFF AdjLMQ/OVA films (i.e., 167.3 ± 44.4 μm). Considering that the distance between the needle tip and the cryogenically cooled surface was fixed during the TFF step, it is likely that the CMC in the AdjLMQ/OVA/$CMC_{1.9\%}$ vaccine made the vaccine droplets difficult to spread upon impact on the cooled surface during the TFF process. It is also possible that for the AdjLMQ/OVA vaccine, without CMC, the sucrose was less prone to collapse during the drying process.

The microscopic structures of the TFF vaccine powders were examined using SEM. The SEM images (Fig. 4**C-F**) (both top view and bottom view) revealed that the TFF AdjLMQ/OVA and AdjLMQ/OVA/$CMC_{1.9\%}$ films were porous. However, the TFF AdjLMQ/OVA/$CMC_{1.9\%}$ sample looked more fibrous than the TFF AdjLMQ/OVA sample (Fig. 4**C vs. 4D**), likely due to the presence of the CMC in the formulation. Moreover, minor phase separation was observed in both samples; the small particles deposited on the sucrose matrix are likely crystals of the buffer salts.

Fig. 5 shows the mDSC profiles of the TFF AdjLMQ/OVA and AdjLMQ/OVA/$CMC_{1.9\%}$ vaccine powders. The glass transition temperature (T_g) of the TFF AdjLMQ/OVA vaccine powder was 6.87 °C, and 32.66 °C for the AdjLMQ/OVA/$CMC_{1.9\%}$ vaccine powder. Because it was reported that freeze-dried samples would crystalize and collapse when being stored at a temperature above their T_g (te Booy et al., 1992), it was concluded that the TFF AdjLMQ/OVA/$CMC_{1.9\%}$ powder could provide better stability while stored at a temperature equal to or below room temperatures. Of course, different sugars and polymers may be included in the powders to further increase their T_g, and thus thermostability, if needed. The mDSC profiles of TFF AdjLMQ/OVA and AdjLMQ/OVA/$CMC_{1.9\%}$ powders both showed a major endotherm peak around 189 °C, which is likely due to the melting of sucrose (Beckett et al., 2006). The presence of melting point indicated that the sucrose might have recrystallized during the heating process. Shown in **Fig. S3** are the total heat flows of TFF AdjLMQ/OVA and AdjLMQ/OVA/$CMC_{1.9\%}$ powders. An exothermic event around 180 °C was identified in both TFF AdjLMQ/OVA and AdjLMQ/OVA/$CMC_{1.9\%}$ powders, and an exothermic event around 60 °C was also present in the TFF AdjLMQ/OVA/$CMC_{1.9\%}$ powder. Sucrose recrystalizes at temperatures greater than 100 °C (Jawad et al., 2018; Roe and Labuza, 2005). Therefore, the exothermic event at around 180 °C is more likely due to the recrystallization of sucrose. The mechanism underlying the smaller peak located left of the main melting endotherm of sucrose in both TFF AdjLMQ/OVA and AdjLMQ/OVA/$CMC_{1.9\%}$ powders is unknown. However, considering that there were several components in the TFF vaccine powders and sucrose is prone to decomposition during the melting process (Lu et al., 2017), the melting endotherm of sucrose could be distorted (Bhandari and Hartel, 2002).

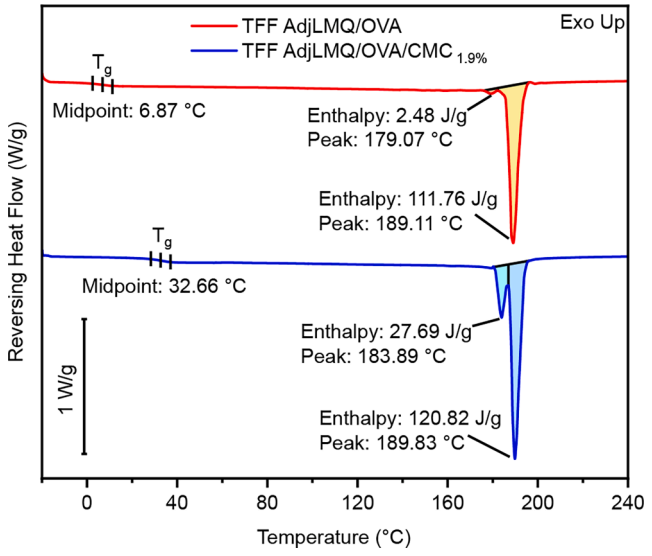

Fig. 5. The mDSC thermograms of the TFF vaccine powders.

3.6. Spraytec analysis of the thin-film freeze-dried AdjLMQ/OVA vaccine powders sprayed with a UDSP nasal device

The AdjLMQ/OVA vaccine powders with 0 or 1.9% w/w CMC were filled into the UDSP nasal device (23.00 ± 1.26 mg per device) and sprayed to characterize the particle size distribution using laser diffraction. The existing FDA's draft guidelines for size distribution characterization by laser diffraction only cover sprayed liquid formulations (U.S. FDA., 2002, 2003). The spray is divided into the initial phase, the fully developed phase, and the dissipation phase. According to the representative transmission profile of AdjLMQ/OVA/$CMC_{1.9\%}$ shown in Fig. 6**A**, the TFF AdjLMQ/OVA vaccine powders sprayed with the UDSP nasal device did not have an obvious fully developed (or stable) phase. Instead, the transmission reached a minimum around 2 ms (ms) after the actuation and then rapidly recovered to the maximum within 14 ms; this result matched the time-course images of the sprayed powder captured by a high-speed camera (Fig. 6**B**). Therefore, 10 snaps of the records with minimum transmission were integrated, which was more representative compared to that in the recommended fully developed phase.

Fig. 7**A and B** show the particle size distribution of the TFF AdjLMQ/OVA and the TFF AdjLMQ/OVA/$CMC_{1.9\%}$ powders, which had a median particle size by volume (Dv(50)) value of 226.3 ± 24.3 μm and 258.2 ± 50.9 μm, respectively. The %V less than 10 μm values, an indication of the percent of particles with diameters lower than 10 μm, for the TFF AdjLMQ/OVA powder and the TFF AdjLMQ/OVA/$CMC_{1.9\%}$ powder were 5.52 ± 2.72% and 4.71 ± 0.77%, respectively (Fig. 7**A, B**).

SEM was used to examine the sprayed powders of the TFF AdjLMQ/OVA and the TFF AdjLMQ/OVA/$CMC_{1.9\%}$ vaccines (Fig. 7**C, D**). The particles of sprayed powders were not uniform, showing a wide size distribution, which agreed with the Spraytec results (Fig. 7**A, B**). Although there were small particles in the sprayed TFF AdjLMQ/OVA powder and TFF AdjLMQ/OVA/$CMC_{1.9\%}$ powder (Fig. 7**C, D**), the contribution of those particles to the volume frequency was not as significant as the large particles. Importantly, since most of the small particles were larger than 10 μm, the risk of the particles entering the lung after intranasal administration in humans is expected to be minimum, indicating that it is suitable to use the UDSP nasal device for intranasal administration of the TFF vaccine powders.

3.7. The plume geometry and spray pattern of the thin-film freeze-dried AdjLMQ/OVA vaccine powders sprayed with the UDSP nasal device

The plume geometry and the spray pattern of the TFF AdjLMQ/OVA vaccine powder were studied after the powder was sprayed using a UDSP nasal device and shown in Fig. 8. The plume angles of the TFF

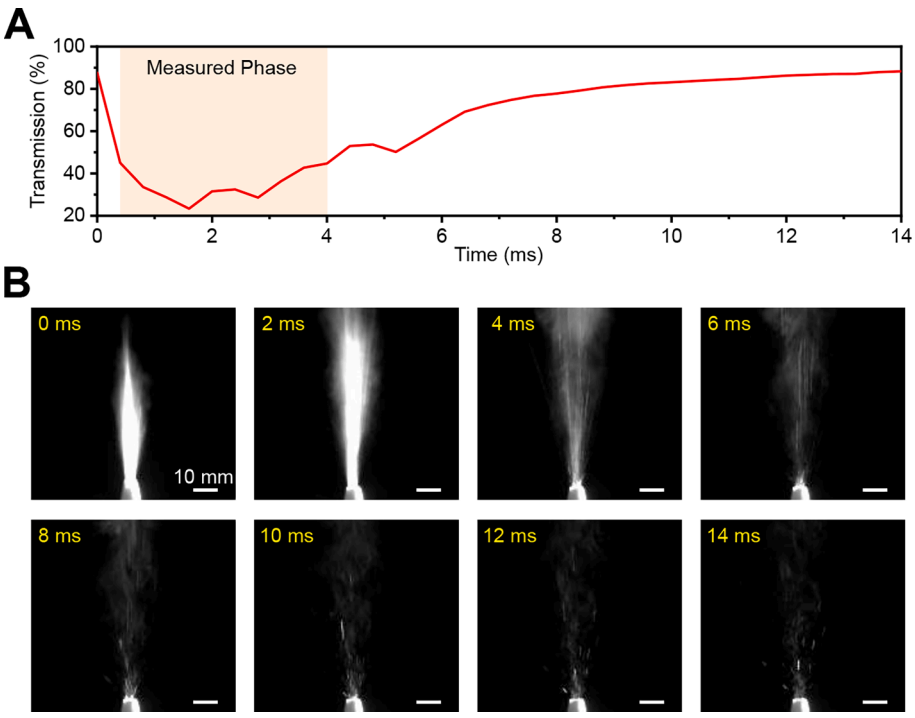

Fig. 6. (A) A representative transmission profile of the TFF AdjLMQ/OVA/$CMC_{1.9\%}$ vaccine powder and (B) the time course images of the TFF AdjLMQ/OVA/$CMC_{1.9\%}$ powder sprayed with the UDSP nasal device.

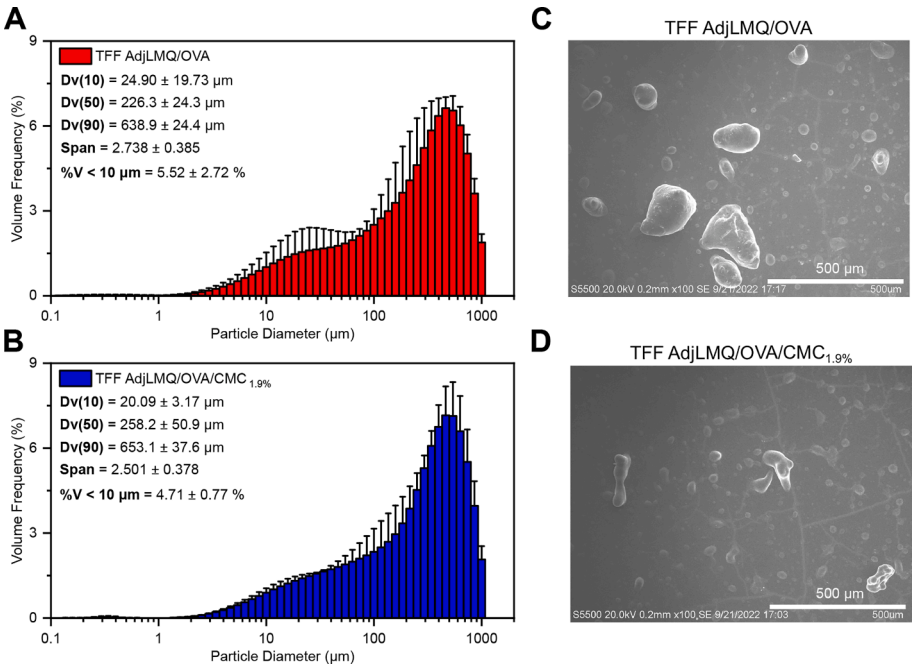

Fig. 7. (A-B) The particle size distribution curves of (A) TFF AdjLMQ/OVA and (B) TFF AdjLMQ/OVA/$CMC_{1.9\%}$ powders sprayed using a UDSP nasal device and determined using a Spraytec spray particle size analyzer. Data are mean ± S.D. (n = 3). (C-D) Representative SEM images of TFF AdjLMQ/OVA powder and TFF AdjLMQ/OVA/$CMC_{1.9\%}$ powder after they were sprayed using a UDSP nasal device.

AdjLMQ/OVA powder and the TFF AdjLMQ/OVA/$CMC_{1.9\%}$ powder were 18.83 ± 2.19° and 19.97 ± 0.75°, respectively. Statistical analysis of the spray pattern shows that the area of the pattern was 434.95 ± 23.22 mm^2 for the TFF AdjLMQ/OVA powder and 415.98 ± 45.88 mm^2 for the TFF AdjLMQ/OVA/$CMC_{1.9\%}$ powder. Both powders had comparable ovality values, i.e., 1.29 ± 0.10 for the TFF AdjLMQ/OVA powder and 1.14 ± 0.06 for the TFF AdjLMQ/OVA/$CMC_{1.9\%}$ powder. Overall, it was concluded that 1.9% w/w CMC in the AdjLMQ/OVA vaccine did not significantly affect the spray pattern and plume geometry of the powder after spraying using the UDSP nasal device.

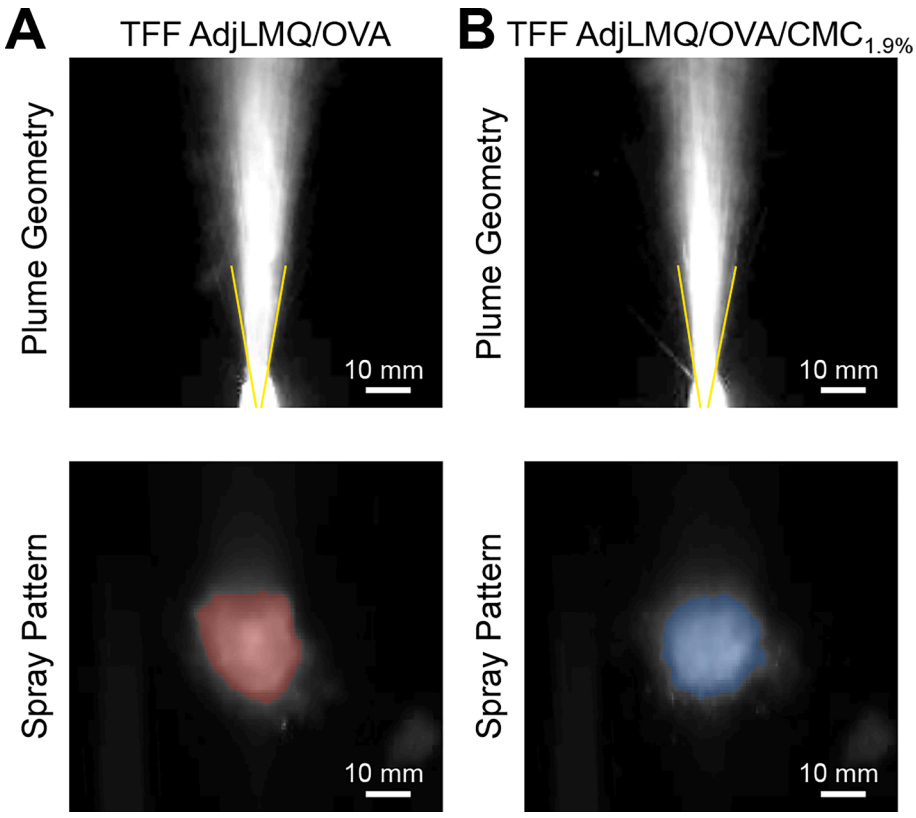

Fig. 8. The plume geometry and spray pattern of the TFF AdjLMQ/OVA and the TFF AdjLMQ/OVA/$CMC_{1.9\%}$ powders after they were sprayed using a UDSP nasal device.

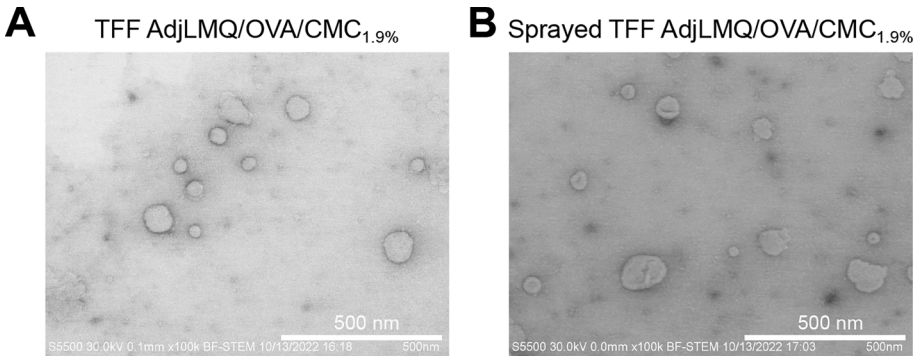

Fig. 9. Representative STEM images of the AdjLMQ/OVA/$CMC_{1.9\%}$ vaccine in TFF AdjLMQ/OVA/$CMC_{1.9\%}$ powder (A) before and (B) after it was sprayed using a UDSP device.

3.8. The integrity of the OVA and the AdjLMQ after the AdjLMQ/OVA vaccine powders were sprayed using the UDSP nasal device

The integrity of the OVA after the TFF AdjLMQ/OVA powder was sprayed using the UDSP nasal device was evaluated using SDS-PAGE. As shown in Fig. 3, a comparison of the OVA bands in lanes IV vs. VI and lanes V vs. VII did not reveal fragmentation or aggregation of the OVA protein in the TFF AdjLMQ/OVA powder and the TFF AdjLMQ/OVA/$CMC_{1.9\%}$ powder. As expected, the OVA protein in the $AS01_B$/OVA vaccine powders was not sensitive to the shear stress associated with spraying them with the UDSP nasal device.

STEM was also used to characterize the AdjLMQ/OVA/$CMC_{1.9\%}$ vaccine in the TFF AdjLMQ/OVA/$CMC_{1.9\%}$ powder before and after it was sprayed with the UDSP nasal device (Fig. 9**A, B**). The liposomes in the TFF AdjLMQ/OVA/$CMC_{1.9\%}$ powder before and after being sprayed with the UDSP nasal device were about 100 nm in diameter. Also, no obvious liposome aggregation was observed after the TFF AdjLMQ/OVA/$CMC_{1.9\%}$ powder was sprayed, indicating that the shear stress associated with the spraying did not compromise the liposomes in the TFF AdjLMQ/OVA/$CMC_{1.9\%}$ vaccine powders. Data from our previous studies showed that subjecting the AdjLMQ/OVA to the thin-film freeze-drying process did not compromise the immunogenicity of the vaccine (AboulFotouh et al., 2022b), and although an animal study is needed to confirm it, we do not expect that adding CMC to vaccine (in less than 2% of the final powder weight) would significantly affect its immunogenicity.

3.9. Deposition patterns of the TFF AdjLMQ/OVA/$CMC_{1.9\%}$ vaccine powder in nasal replica casts

The TFF AdjLMQ/OVA/$CMC_{1.9\%}$ powder was manually loaded into the UDSP nasal device at 22.92 ± 1.82 mg (n = 30). After actuation, the

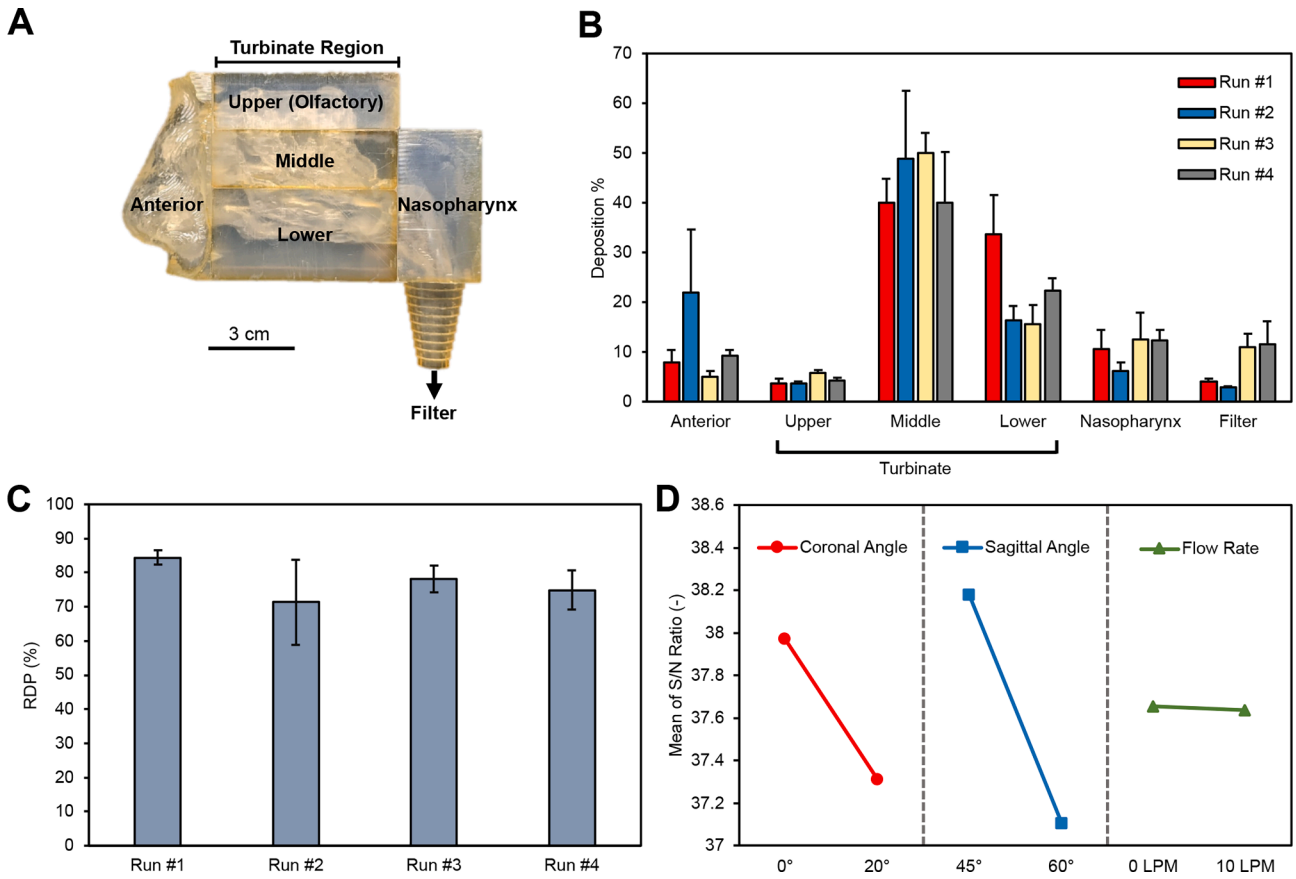

Fig. 10. Deposition patterns of TFF AdjLMQ/OVA/CMC$_{1.9\%}$ vaccine powder after being sprayed into a nasal cast based on a 48-year-old male. (A) A digital image of the nasal cast with different regions labeled. (B) The deposition patterns of the TFF AdjLMQ/OVA/CMC$_{1.9\%}$ powder in different regions. The parameters were designed with the Taguchi array method. (C) The regional deposition efficiency (RDP) of the 4 conditions in the middle and lower turbinate and the nasopharynx regions. (D) The signal to noise (S/N) ratio of each parameter at different levels. Data in B-C are mean ± S.D. (n = 3).

delivered amount of the TFF AdjLMQ/OVA/CMC$_{1.9\%}$ powder was 21.54 ± 1.72 mg. The averaged delivery efficiency was 94.11 ± 5.13%. In this study, an airflow of 10 LPM was chosen to simulate shallow breathing for the 48-year-old male model according to a previous study (Warnken et al., 2018). A reduced airflow of 5 LPM was chosen for the 7-year-old female model. Xi et al. applied the airflows of 3 and 30 LPM to simulate the sedentary and heavily active breathing conditions of a 5-year-old male, respectively (Xi et al., 2011).

The deposition pattern of the TFF AdjLMQ/OVA/CMC$_{1.9\%}$ powder after being sprayed into the nasal cast based on the CT scan of a 48-year-old male is shown in Fig. 10**A-B**. The recovery rate/percent of the TFF AdjLMQ/OVA/CMC$_{1.9\%}$ vaccine powder in the 48-year-old male nasal cast ranged from 82.3% to 88.4% (Fig. S4**A**). In all the conditions, the majority of the TFF powder was deposited in the middle and lower turbinate and the nasopharynx regions. When an air flow of 10 LPM was applied to the nasal cast, the deposition percentage in the nasopharynx region and the filter increased, as expected. For a nasal vaccine, it is not ideal for the vaccine to travel beyond the nasal cavity after administration. However, the powder collected on the filter will not necessarily travel to the deep lung. Instead, the filter more likely represents the tracheal region. In fact, we have previously showed that the aerosol performance of the same vaccine powder without CMC is not desirable for lung delivery by oral inhalation and the TFF process parameters needed to be modified to make powders with good aerosol properties of lung delivery (AboulFotouh and Cui, unpublished data). The percentage deposited in the upper turbinate region where the olfactory bulb resides was less than 10% in all the conditions, indicating that the exposure of the vaccine powder to the olfactory bulb can be minimized by spraying the TFF vaccine powder with the UDSP nasal device. As shown in Fig. 10**C**, the RDP, percent deposition in the middle and lower turbinate and the nasopharynx regions, of Run #1 had the highest value of 84.4%, and the Run #2 showed the lowest value of 71.3%. To evaluate the effect of each parameter on the RDP, the S/N ratios were calculated. Since a higher S/N ratio will lead to a higher RDP, it was concluded that the optimal condition for the RDP in the nasal cast based on a 48-year-old male is: 0° for the coronal angle, 45° for the sagittal angle, and 0 LPM for the flow rate, which is the same as Run #1 (Fig. 10**D**). Finally, since the difference of the S/N ratio between two levels indicates the impact of the parameter on the RDP, it was concluded that the order of the impact on RDP was sagittal angle > coronal angle > flow rate.

The deposition pattern of the TFF AdjLMQ/OVA/CMC$_{1.9\%}$ powder after being sprayed into a nasal cast based on the CT scan of a 7-year-old female is shown in Fig. 11**A-B**. The recovery rate of the TFF AdjLMQ/OVA/CMC$_{1.9\%}$ vaccine powder in the 7-year-old female nasal cast ranged from 79.3% to 93.7 % (Fig. S4**B**). Most of the TFF AdjLMQ/OVA/CMC$_{1.9\%}$ powder was also deposited in the middle and lower turbinate regions and the nasopharynx region. Compared to the results generated using the adult nasal cast, the differences between different conditions were more significant in the child nasal cast. For example, Run #1 resulted in the highest deposition percentage in the nasopharynx region (Fig. 11**B**), which was desirable for intranasal immunization. This was likely due to the smaller size/depth of the nasal cavity in children, making the effect of these conditions more pronounced. The RDP among 4 conditions ranged from 75.8% to 88.8% (Fig. 11**C**), which were generally greater than that of the adult nasal cast. The calculated S/N ratios for all parameters indicated that the optimal condition for the deposition pattern was also: 0° for the coronal angle, 45° for the sagittal angle, and 0 LPM for the flow rate, which is the same as Run #1

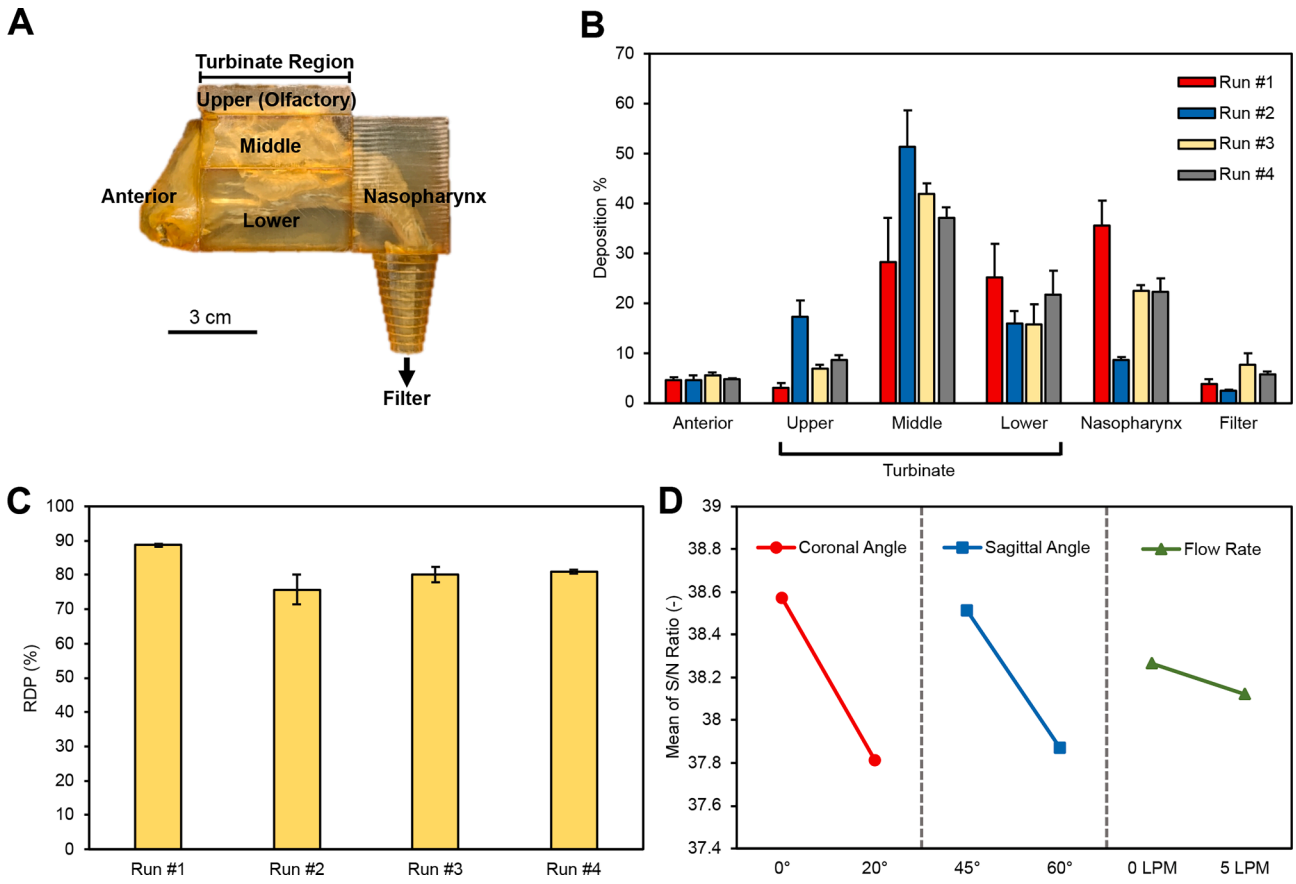

Fig. 11. Deposition pattern of TFF AdjLMQ/OVA/$CMC_{1.9\%}$ vaccine powder after being sprayed into a nasal cast based on a 7-year-old female. (A) A digital image of the nasal cast with different regions labeled. (B) The deposition patterns of the TFF AdjLMQ/OVA/$CMC_{1.9\%}$ powder in different regions. The parameters were designed with the Taguchi array method. (C) The regional deposition efficiency (RDP) of the 4 conditions in the middle and lower turbinate and the nasopharynx regions. (D) The S/N ratio of each parameter at different levels. Data in B-C are mean ± S.D. (n = 3).

(Fig. 11**D**). Different from the adult nasal cast, however, the order of the impact on RDP was coronal angle > sagittal angle > flow rate.

Taken together, data in Fig. 10 and Fig. 11 showed that in both adult and child nasal casts, the optimal condition to deliver the TFF AdjLMQ/OVA/$CMC_{1.9\%}$ vaccine powder to the middle and lower turbinate and the nasopharynx regions was 0° for the coronal angle, 45° for the sagittal angle, and 0 LPM for the flow rate. The insertion depth is expected to also significantly affect the deposition pattern of the TFF vaccine powder sprayed using the UDSP nasal device (Gao et al., 2020). In the present study, the insertion depth for the adult nasal cast was 0.5 cm, and 0.4 cm for the child nasal cast, so that all the parameters in the Taguchi L4 orthogonal array in Table 1 can be accommodated. Due to the rigid structure of the 3D-printed nasal casts, the insertion depth could not be adjusted in a large interval. Further optimization of the insertion depth may be considered in the future.

Fig. 12**A** showed the deposition percentages of the TFF AdjLMQ/OVA/$CMC_{1.9\%}$ vaccine powder directly in the nasopharynx region of a 48-year-old male nasal cast in 4 different runs. The S/N ratios in Fig. 12**B** indicated that the optimal condition for the TFF vaccine powder to be delivered directly to the nasopharynx region of the nasal cast based on the 48-year-old male is: 0° for the coronal angle, 45° for the sagittal angle, and 10 LPM for the flow rate. The deposition pattern of the TFF AdjLMQ/OVA/$CMC_{1.9\%}$ vaccine powder at the optimal condition identified above is shown in Fig. 12**C**. The percentage of the powder deposited directly in the nasopharynx region was 15.09 ± 4.05%.

Fig. 12**D** showed the deposition percentages of the TFF AdjLMQ/OVA/$CMC_{1.9\%}$ vaccine powder directly in the nasopharynx region of the 7-year-old female nasal cast in 4 different runs. The S/N ratios in Fig. 12**E** indicated that the optimal condition for the TFF vaccine powder to be delivered directly to the nasopharynx region of the nasal cast based on the 7-year-old female is 0° for the coronal angle, 45° for the sagittal angle, and 5 LPM for the flow rate. The deposition pattern of the TFF AdjLMQ/OVA/$CMC_{1.9\%}$ vaccine powder at the optimal condition identified above is shown in Fig. 12**F**. The percentage of the powder deposited directly in the nasopharynx region was 34.33 ± 3.77%, which is not significantly different from the deposition percentage in the nasopharynx region at 0 LPM flow rate (i.e., 35.49 ± 5.14%), likely due to the weak correction between deposition in the nasopharynx regions and the flow rate (Fig. 12**E**). Meanwhile, the deposition percentage in the filter increased from 3.73 ± 1.01% to 15.73 ± 2.20%. Therefore, if one only considers the TFF AdjLMQ/OVA/$CMC_{1.9\%}$ vaccine powder that is directly delivered into the nasopharynx region, where the Waldeyer's ring is located, then applying a flow rate, similar to applying the vaccine to a human subject while the human subject is inhaling, is expected to be beneficial in adults, but not in children, and there is also an increased chance for the powder to travel beyond the nasopharynx region into the trachea. Direct deposition of a vaccine to the nasopharynx region is important as the vaccine is expected to have a higher chance of reaching the lymphoid tissues (i.e., adenoids and tubal tonsils) in the Waldeyer's ring. If the vaccine is deposited in the middle and lower turbinates, it may ultimately reach the naso-oropharynx region by being carried by the mucous blanket posterior movement, but the lymphoid tissues in the naso-oropharynx need to efficiently 'fish out' the vaccine or antigens bound to the mucus.

The results reported in this study showed that a protein antigen-based vaccine that is adjuvanted with the liposomal AdjLMQ adjuvant and contains CMC as a mucoadhesive agent could be converted into a dry powder using the thin-film freeze-drying technology and then

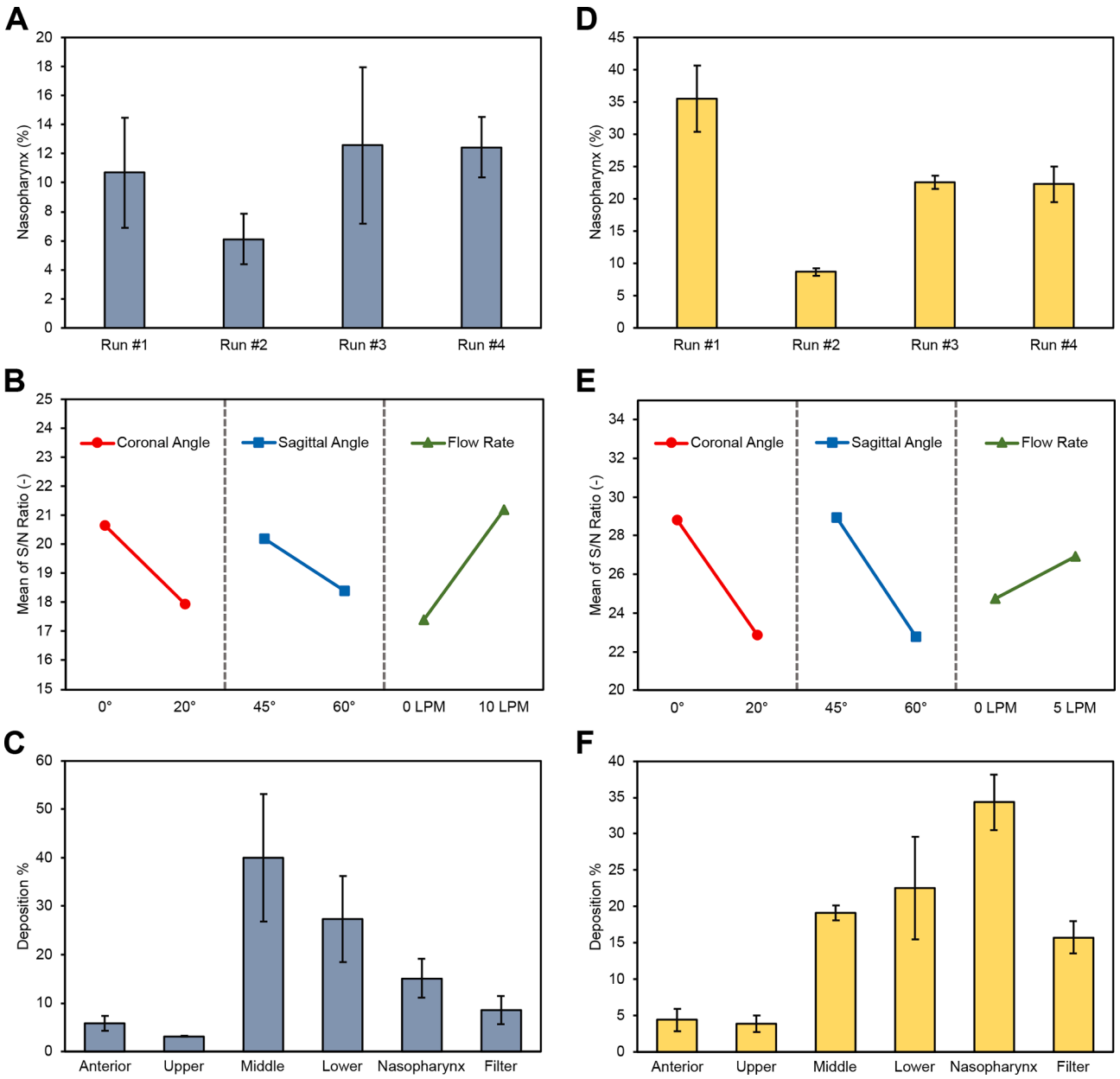

Fig. 12. Optimization of the nasopharynx deposition. (A) The deposition percentage of the TFF AdjLMQ/OVA/$CMC_{1.9\%}$vaccine powder in the nasopharynx region of a 48-year-old male nasal cast. (B) The S/N ratio of each parameter at different levels for the 48-year-old male nasal cast. (C) The deposition patterns of the TFF AdjLMQ/OVA/$CMC_{1.9\%}$ powder in the 48-year-old male nasal cast at the following condition: coronal angle = 0°, sagittal angle = 45°, flow rate = 10 LPM. (D) The deposition percentage of the TFF AdjLMQ/OVA/$CMC_{1.9\%}$vaccine powder in the nasopharynx region of a 7-year-old female nasal cast. (B) The S/N ratio of each parameter at different levels for the 7-year-old female nasal cast. (C) The deposition patterns of the TFF AdjLMQ/OVA/$CMC_{1.9\%}$ powder in the 7-year-old female nasal cast at the following condition: coronal angle = 0°, sagittal angle = 45°, flow rate = 5 LPM.

delivered to the desired regions in nasal replica casts 3D printed based on the CT-scan images of human noses using the UDSP nasal device. Besides the AdjLMQ-adjuvanted vaccines, thin-film freeze-drying technology has been successfully applied to various other types of vaccines, including vaccines adjuvanted with aluminum salt (Alzhrani et al., 2021; Li et al., 2015; Thakkar et al., 2018), MF59 or AddaVax (Aboul-Fotouh et al., 2022a), plasmid DNA vaccine (Xu et al., 2022), viral vector-based vaccines (unpublished data), and messenger RNA-lipid nanoparticle vaccines (unpublished data). In addition, both Gram-positive and Gram-negative bacteria in suspension can be converted to dry powders using the thin-film freeze-drying technology (Wang et al., 2022). Therefore, it is expected that various other types of vaccines can be administered intranasally as thin-film freeze-dried powders using the UDSP nasal device to target the vaccines to the lymphoid tissues in the nasopharynx region in humans. Of course, for different vaccines, additional optimization of the formulation and critical process parameters will likely be needed.

For decades, there has been a strong interest in developing intranasal vaccines. However, as aforementioned, only a few nasal vaccines have received regulatory approval for human use around the world. Many nasal vaccine candidates that are safe and efficacious in preclinical studies often fail to move beyond phase 1 in clinical testing (Cai et al., 2022). For example, the ChAdOx1 nCoV-19 simian adenovirus-based COVID-19 vaccine that was effective in hamsters and non-human primates failed to elicit consistent immune responses in human volunteers when given intranasally (Madhavan et al., 2022). The authors posited that the dosage form and the device used to administer the vaccine, which were not optimized for intranasal vaccination in humans, may

have contributed, at least in part, to the weak and inconsistent immune responses seen (Madhavan et al., 2022), underscoring the significance of optimizing vaccine formulation and delivery device in nasal vaccine development.

Nasal vaccines that are currently approved for human use around the world are liquid suspension or freeze-dried powder that must be reconstituted before administration. They are sprayed into the nostrils using a nasal spray system such as the BD Accuspray™. Intranasal immunization using a vaccine dry powder is appealing, but a technology that can transform vaccines from liquid to a dry powder suitable for intranasal delivery, while preserving the physical and chemical properties and the immunogenicity of the vaccines is needed. Similarly, a dry powder delivery system that can deliver the vaccine powder to the desired region(s) of the human nasal cavity is also required because there has not been an approved nasal dry powder vaccine for human use yet. Since many intranasal vaccines failed to move beyond phase 1 clinical trials (Cai et al., 2022; Xu et al., 2021b), the formulation of a vaccine intended for intranasal administration must be optimized, and only a device that can efficiently target the vaccine to the desired region (s) in the nasal cavity should be chosen. As aforementioned, in children and adults, the Waldeyer's ring in the naso-oropharynx region is the key lymphoid tissue in the nasal cavity. Therefore, it is ideal to deliver a vaccine powder directly to the nasopharynx region. If the vaccine is delivered in the posterior nasal cavity and binds to the mucus, then it may be carried to the naso-oropharynx region by the mucous blanket posterior movement by means of ciliary clearance, wherein the vaccine may be taken up by the lymphoid tissues in the Waldeyer's ring or cleared through the throat to the stomach and then degraded or deactivated there (Sahin-Yilmaz and Naclerio, 2011). It is possible, or perhaps probable, that some cells in the epithelium of the posterior nasal cavity covered by the mucous layer may be able to take up the vaccine or the antigens, but the vaccine/antigen must penetrate through the mucous layer quickly and efficiently, and then bind and preferably be taken up by cells in the underling epithelium, as the mucous blanket posterior movement can clear inhaled particles from the nasal cavity in 10–20 min (Sahin-Yilmaz and Naclerio, 2011).

A vaccine that is deposited in the region that is anterior to the lower turbinate will be transported anterior out of the nostrils. Testing vaccine powders and delivery devices directly in human subjects is ideal, but less practical. Nasal replica casts 3D printed based on the CT scan images of the noses of humans, such as the nasal replica casts used in the present study and the idealized nasal replica (Chen et al., 2020), provide an attractive alternative for vaccine powder optimization and dry powder delivery device selection. Vaccine formulations and delivery devices selected based on nasal replica casts can then be validated in humans to verify the deposition of the vaccine powder to desired regions or sites before initiating clinical trials to test the safety and efficacy of new vaccine candidates.

4. Conclusions

It is concluded that it is feasible to apply the thin-film freeze-drying technology to convert vaccines such as the AdjLMQ-adjuvanted OVA model vaccine with a suitable mucoadhesive agent such as CMC into dry powders, and the resultant vaccine powders can be delivered to the desired regions of 3D printed human nasal casts using the Aptar Pharma's UDSP nasal device. The type of the mucoadhesive agent and its concentration were critical to preserve the physical properties of the vaccine and the integrity of the antigen after the vaccine was subjected to the thin-film freeze-drying. The mucoadhesive agent also affected the powder properties of the vaccine powder. When sprayed using the UDSP nasal device, the vaccine powders prepared using thin-film freeze-drying showed desirable particle size distribution, spray pattern and plume geometry. Importantly, spraying the vaccine powder with the UDSP nasal device did not negatively affect the antigen and the adjuvant. Finally, evaluation of the deposition patterns of TFF AdjLMQ/OVA/$CMC_{1.9\%}$ powder in both adult and child nasal replica casts showed that the optimal delivery parameters for both nasal casts were: 0° for the coronal angle, 45° for the sagittal angle, and 0 LPM for the flow rate, and more than 80% of the powders were deposited in the middle and lower turbinate and the nasopharynx regions. If only the nasopharynx region is considered, then applying a flow rate was beneficial.

CRediT authorship contribution statement

Yu-Sheng Yu: Conceptualization, Methodology, Investigation, Visualization, Formal analysis, Writing - original draft. **Khaled AboulFotouh:** Methodology, Investigation. **Haiyue Xu:** Methodology, Investigation. **Gerallt Williams:** Conceptualization, Resources, Writing – review & editing. **Julie Suman:** Conceptualization, Resources, Writing – review & editing. **Chris Cano:** Conceptualization, Resources, Writing – review & editing. **Zachary N. Warnken:** Methodology, Investigation, Writing – review & editing. **Kevin C.-W. Wu:** Writing – review & editing, Funding acquisition. **Robert O. Williams:** Resources, Writing – review & editing, Funding acquisition. **Zhengrong Cui:** Conceptualization, Resources, Validation, Writing – review & editing, Supervision, Funding acquisition.

Declaration of Competing Interest

The authors declare the following financial interests/personal relationships which may be considered as potential competing interests: Z Cui reports a relationship with TFF Pharmaceuticals, Inc. that includes equity or stocks and research funding. RO Williams III reports a relationship with TFF Pharmaceuticals, Inc. that includes consulting or advisory, equity or stocks, and research funding. Z Cui and RO Williams III report a relationship with Via Therapeutics, LLC that includes equity. H Xu reports a relationship with TFF Pharmaceuticals, Inc. that includes consulting. Financial conflict of interest management plans are available at UT Austin.

Data availability

Data will be made available on request.

Acknowledgements

Z Cui and RO Williams III report financial support from TFF Pharmaceuticals, Inc. The UDSP device was generously provided by Aptar Pharma. YS Yu was supported in part by the Y.L. Lin Hung Tai Education Foundation, and YS Yu and KCW Wu report support from the Taiwan Ministry of Science and Technology (award #: 111-2628-E-002-008). K AboulFotouh was supported in part by an Egyptian Government Fellowship. We thank Dr. Hugh Smyth in the College of Pharmacy at UT Austin for the laser sheet system used to acquire the spray pattern and plume geometry data.

The graphical abstract was created with BioRender.com and adopted from "Head and Neck Anatomy", by BioRender.com (2020). Retrieved from https://app.biorender.com/biorender-templates.

Appendix A. Supplementary data

Supplementary data to this article can be found online at https://doi.org/10.1016/j.ijpharm.2023.122990.

References

AboulFotouh, K., Uno, N., Xu, H., Moon, C., Sahakijpijarn, S., Christensen, D.J., Davenport, G.J., Cano, C., Ross, T.M., Williams Iii, R.O., Cui, Z., 2022a. Formulation of dry powders of vaccines containing MF59 or AddaVax by Thin-Film Freeze-Drying: Towards a dry powder universal flu vaccine. Int. J. Pharm. 624, 122021 https://doi.org/10.1016/j.ijpharm.2022.122021.

AboulFotouh, K., Xu, H., Moon, C., Williams 3rd, R.O., Cui, Z., 2022b. Development of (inhalable) dry powder formulations of AS01(B)-containing vaccines using Thin-Film Freeze-Drying. Int. J. Pharm. 622, 121825 https://doi.org/10.1016/j.ijpharm.2022.121825.

Alzhrani, R.F., Xu, H., Moon, C., Suggs, L.J., Williams 3rd, R.O., Cui, Z., 2021. Thin-Film Freeze-Drying is a viable method to convert vaccines containing aluminum salts from liquid to dry powder. Methods Mol. Biol. 2183, 489–498. https://doi.org/10.1007/978-1-0716-0795-4_27.

Baldridge, J.R., Yorgensen, Y., Ward, J.R., Ulrich, J.T., 2000. Monophosphoryl lipid A enhances mucosal and systemic immunity to vaccine antigens following intranasal administration. Vaccine 18, 2416–2425. https://doi.org/10.1016/S0264-410X(99)00572-1.

Beckett, S.T., Francesconi, M.G., Geary, P.M., Mackenzie, G., Maulny, A.P., 2006. DSC study of sucrose melting. Carbohydr. Res. 341, 2591–2599. https://doi.org/10.1016/j.carres.2006.07.004.

Bhandari, B.R., Hartel, R.W., 2002. Co-crystallization of sucrose at high concentration in the presence of glucose and fructose. J. Food Sci. 67, 1797–1802. https://doi.org/10.1111/j.1365-2621.2002.tb08725.x.

Birkhoff, M., Leitz, M., Marx, D., 2009. Advantages of intranasal vaccination and considerations on device selection. Indian J. Pharm. Sci. 71, 729–731.

Cai, L., Xu, H., Cui, Z., 2022. Factors limiting the translatability of rodent model-based intranasal vaccine research to humans. AAPS PharmSciTech 23, 191. https://doi.org/10.1208/s12249-022-02330-9.

Chavda, V.P., Vora, L.K., Pandya, A.K., Patravale, V.B., 2021. Intranasal vaccines for SARS-CoV-2: From challenges to potential in COVID-19 management. Drug Discov. Today 26, 2619–2636. https://doi.org/10.1016/j.drudis.2021.07.021.

Chen, J.Z., Kiaee, M., Martin, A.R., Finlay, W.H., 2020. In vitro assessment of an idealized nose for nasal spray testing: Comparison with regional deposition in realistic nasal replicas. Int. J. Pharm. 582, 119341 https://doi.org/10.1016/j.ijpharm.2020.119341.

Covaciu, M., Olaru, F., Petrescu, I., 2004. Ovalbumin isoforms - purification and denaturation/renaturation studies. Analele Stiintifice ale Universitatii "Alexandru Ioan Cuza" din Iasi Sec. II a. Genetica si Biologie Moleculara 5.

Davis, S.S., 2001. Nasal vaccines. Adv. Drug Deliv. Rev. 51, 21–42. https://doi.org/10.1016/S0169-409X(01)00162-4.

Debertin, A.S., Tschernig, T., Tönjes, H., Kleemann, W.J., Tröger, H.D., Pabst, R., 2003. Nasal-associated lymphoid tissue (NALT): frequency and localization in young children. Clin. Exp. Immunol. 134, 503–507. https://doi.org/10.1111/j.1365-2249.2003.02311.x.

Dekina, S., Romanovska, I., Ovsepyan, A., Tkach, V., Muratov, E., 2016. Gelatin/carboxymethyl cellulose mucoadhesive films with lysozyme: Development and characterization. Carbohydr. Polym. 147, 208–215. https://doi.org/10.1016/j.carbpol.2016.04.006.

Engstrom, J.D., Lai, E.S., Ludher, B.S., Chen, B., Milner, T.E., Williams 3rd, R.O., Kitto, G. B., Johnston, K.P., 2008. Formation of stable submicron protein particles by thin film freezing. Pharm. Res. 25, 1334–1346. https://doi.org/10.1007/s11095-008-9540-4.

Flood, A., Estrada, M., McAdams, D., Ji, Y., Chen, D., 2016. Development of a freeze-dried, heat-stable influenza subunit vaccine formulation. PLoS One 11, e0164692.

Gao, M., Shen, X., Mao, S., 2020. Factors influencing drug deposition in thenasal cavity upon delivery via nasal sprays. J. Pharm. Investig. 50, 251–259. https://doi.org/10.1007/s40005-020-00482-z.

Gasparini, C., Acunzo, M., Biuso, A., Roncaglia, S., Migliavacca, F., Borriello, C.R., Bertolini, C., Allen, M.R., Orenti, A., Boracchi, P., Zuccotti, G.V., 2021. Nasal spray live attenuated influenza vaccine: the first experience in Italy in children and adolescents during the 2020–21 season. Ital. J. Pediatr. 47, 225. https://doi.org/10.1186/s13052-021-01172-8.

Ghani, J.A., Choudhury, I.A., Hassan, H.H., 2004. Application of Taguchi method in the optimization of end milling parameters. Mater. Process. Technol. 145, 84–92. https://doi.org/10.1016/S0924-0136(03)00865-3.

Grabovac, V., Guggi, D., Bernkop-Schnürch, A., 2005. Comparison of the mucoadhesive properties of various polymers. Adv. Drug Deliv. Rev. 57, 1713–1723. https://doi.org/10.1016/j.addr.2005.07.006.

Hufnagel, S., Sahakijpijarn, S., Moon, C., Cui, Z., Williams III, R.O., 2022. The development of thin-film freezing and its application to improve delivery of biologics as dry powder aerosols. Kona Powder Part. J. 2022010.

Jawad, R., Elleman, C., Martin, G.P., Royall, P.G., 2018. Crystallisation of freeze-dried sucrose in model mixtures that represent the amorphous sugar matrices present in confectionery. Food Funct. 9, 4621–4634. https://doi.org/10.1039/C8FO00729B.

Kesavan, K., Nath, G., Pandit, J.K., 2010. Sodium alginate based mucoadhesive system for gatifloxacin and its in vitro antibacterial activity. Sci. Pharm. 78, 941–957. https://doi.org/10.3797/scipharm.1004-24.

Li, X., Thakkar, S.G., Ruwona, T.B., Williams, R.O., Cui, Z., 2015. A method of lyophilizing vaccines containing aluminum salts into a dry powder without causing particle aggregation or decreasing the immunogenicity following reconstitution. J. Controlled Release 204, 38–50. https://doi.org/10.1016/j.jconrel.2015.02.035.

Lu, Y., Thomas, L.C., Jerrell, J.P., Cadwallader, K.R., Schmidt, S.J., 2017. Investigating the thermal decomposition differences between beet and cane sucrose sources. J. Food Meas. Charact. 11, 1640–1653. https://doi.org/10.1007/s11694-017-9544-z.

Madhavan, M., Ritchie, A.J., Aboagye, J., Jenkin, D., Provstgaad-Morys, S., Tarbet, I., Woods, D., Davies, S., Baker, M., Platt, A., Flaxman, A., Smith, H., Belij-Rammerstorfer, S., Wilkins, D., Kelly, E.J., Villafana, T., Green, J.A., Poulton, I., Lambe, T., Hill, A.V.S., Ewer, K.J., Douglas, A.D., 2022. Tolerability and immunogenicity of an intranasally-administered adenovirus-vectored COVID-19 vaccine: An open-label partially-randomised ascending dose phase I trial. eBioMedicine, 104298. https://doi.org/10.1016/j.ebiom.2022.104298.

Ortiz, J.R., Goswami, D., Lewis, K.D., Sharmeen, A.T., Ahmed, M., Rahman, M., Rahman, M.Z., Feser, J., Neuzil, K.M., Brooks, W.A., 2015. Safety of Russian-backbone seasonal trivalent, live-attenuated influenza vaccine in a phase II randomized placebo-controlled clinical trial among children in urban Bangladesh. Vaccine 33, 3415–3421. https://doi.org/10.1016/j.vaccine.2015.04.048.

Overhoff, K.A., Johnston, K.P., Tam, J., Engstrom, J., Williams, R.O., 2009. Use of thin film freezing to enable drug delivery: A review. J. Drug Deliv. Sci. Technol. 19, 89–98. https://doi.org/10.1016/S1773-2247(09)50016-0.

Roe, K., Labuza, T., 2005. Glass transition and crystallization of amorphous trehalose-sucrose mixtures. Int. J. Food Prop. 8, 559–574. https://doi.org/10.1080/10942910500269824.

Sahin-Yilmaz, A., Naclerio, R.M., 2011. Anatomy and physiology of the upper airway. Proc. Am. Thorac. Soc. 8, 31–39. https://doi.org/10.1513/pats.201007-050RN.

Saito, S., Ainai, A., Suzuki, T., Harada, N., Ami, Y., Yuki, Y., Takeyama, H., Kiyono, H., Tsukada, H., Hasegawa, H., 2016. The effect of mucoadhesive excipient on the nasal retention time of and the antibody responses induced by an intranasal influenza vaccine. Vaccine 34, 1201–1207. https://doi.org/10.1016/j.vaccine.2016.01.020.

Sasaki, S., Hamajima, K., Fukushima, J., Ihata, A., Ishii, N., Gorai, I., Hirahara, F., Mohri, H., Okuda, K., 1998a. Comparison of intranasal and intramuscular immunization against human immunodeficiency virus type 1 with a DNA-monophosphoryl lipid A adjuvant vaccine. Infect. Immun. 66, 823–826. https://doi.org/10.1128/IAI.66.2.823-826.1998.

Sasaki, S., Sumino, K., Hamajima, K., Fukushima, J., Ishii, N., Kawamoto, S., Mohri, H., Kensil, C.R., Okuda, K., 1998b. Induction of systemic and mucosal immune responses to human immunodeficiency virus type 1 by a DNA vaccine formulated with QS-21 saponin adjuvant via intramuscular and intranasal routes. J. Virol. 72, 4931–4939. https://doi.org/10.1128/JVI.72.6.4931-4939.1998.

Sato-Kaneko, F., Yao, S., Lao, F.S., Sako, Y., Jin, J., Shukla, N.M., Cottam, H.B., Chan, M., Belsuzarri, M.M., Carson, D.A., Hayashi, T., 2022. A dual adjuvant system for intranasal boosting of local and systemic immunity for influenza vaccination. Vaccines 10, 1694. https://doi.org/10.3390/vaccines10101694.

Sigma-Aldrich, 2021. FluoroTag™ FITC Conjugation Kit. https://www.sigmaaldrich.com/deepweb/assets/sigmaaldrich/product/documents/364/319/fitc1bul.pdf (accessed 26 Jan 2023).

Sogias, I.A., Williams, A.C., Khutoryanskiy, V.V., 2008. Why is chitosan mucoadhesive? Biomacromolecules 9, 1837–1842. https://doi.org/10.1021/bm800276d.

Suryadevara, M., Domachowske, J.B., 2014. Quadrivalent influenza vaccine in the United States. Hum Vaccin Immunother 10, 596–599. https://doi.org/10.4161/hv.27115.

te Booy, M.P., de Ruiter, R.A., de Meere, A.L., 1992. Evaluation of the physical stability of freeze-dried sucrose-containing formulations by differential scanning calorimetry. Pharm Res 9, 109–114. https://doi.org/10.1023/a:1018944113914.

Thakkar, S.G., Warnken, Z.N., Alzhrani, R.F., Valdes, S.A., Aldayel, A.M., Xu, H., Williams, R.O., Cui, Z., 2018. Intranasal immunization with aluminum salt-adjuvanted dry powder vaccine. Journal of Controlled Release 292, 111–118. https://doi.org/10.1016/j.jconrel.2018.10.020.

ThermoFisher Scientific, n.d. Ovalbumin Polyclonal Antibody, HRP (PA1-196-HRP). https://www.thermofisher.com/antibody/product/Ovalbumin-Antibody-Polyclonal/PA1-196-HRP (accessed 26 Jan 2023).

Trenkel, M., Scherließ, R., 2021. Nasal powder formulations: in-vitro characterisation of the impact of powders on nasal residence time and sensory effects. Pharmaceutics 13, 385.

U.S. FDA., 2002. Nasal Spray and Inhalation Solution, Suspension, and Spray Drug Products — Chemistry, Manufacturing, and Controls Documentation.

U.S. FDA., 2003. Bioavailability and Bioequivalence Studies for Nasal Aerosols and Nasal Sprays for Local Action, in: Research, C.f.D.E.a. (Ed.).

Wang, J.-L., Kuang, M., Xu, H., Williams, R.O., Cui, Z., 2022. Accelerated mass transfer from frozen thin films during thin-film freeze-drying. bioRxiv, 2022.2004.2016.488553. https://doi.org/10.1101/2022.04.16.488553.

Wang, J.L., Hanafy, M.S., Xu, H., Leal, J., Zhai, Y., Ghosh, D., Williams III, R.O., David Charles Smyth, H., Cui, Z., 2021. Aerosolizable siRNA-encapsulated solid lipid nanoparticles prepared by thin-film freeze-drying for potential pulmonary delivery. Int. J. Pharm. 596, 120215 https://doi.org/10.1016/j.ijpharm.2021.120215.

Warnken, Z.N., Smyth, H.D.C., Davis, D.A., Weitman, S., Kuhn, J.G., Williams, R.O., 2018. Personalized medicine in nasal delivery: The use of patient-specific administration parameters to improve nasal drug targeting using 3D-printed nasal replica casts. Mol. Pharm. 15, 1392–1402. https://doi.org/10.1021/acs.molpharmaceut.7b00702.

Xi, J., Si, X., Kim, J.W., Berlinski, A., 2011. Simulation of airflow and aerosol deposition in the nasal cavity of a 5-year-old child. J. Aerosol Sci. 42, 156–173. https://doi.org/10.1016/j.jaerosci.2010.12.004.

Xu, H., Bhowmik, T., Gong, K., Huynh, T.N.A., Williams, R.O., Cui, Z., 2021a. Thin-film freeze-drying of a bivalent Norovirus vaccine while maintaining the potency of both antigens. Int. J. Pharm. 609, 121126 https://doi.org/10.1016/j.ijpharm.2021.121126.

Xu, H., Cai, L., Hufnagel, S., Cui, Z., 2021b. Intranasal vaccine: Factors to consider in research and development. Int. J. Pharm. 609, 121180 https://doi.org/10.1016/j.ijpharm.2021.121180.

Xu, H., Moon, C., Sahakijpijarn, S., Dao, H.M., Alzhrani, R.F., Wang, J.-l., Williams, R.O., Cui, Z., 2022. Aerosolizable plasmid DNA dry powders engineered by thin-film freezing. bioRxiv, 2022.2010.2003.510625. https://doi.org/10.1101/2022.10.03.510625.